Electronic Supplementary Material (ESI) for Journal of Materials Chemistry B.

Supporting Information for:

In vivo two-photon imaging/excited photothermal therapy strategy of a silver-nanohybrid

Ze Huang, Li Gao, Lin Kong, Hui-Hui Zhang, Jia-Xiang Yang, Lin Li

Contents

S1 Instruments and measurements

^{1}H NMR, ^{13}C NMR were measured on Bruker Avance 400 MHz spectrometer with tetramethylsilane (TMS) as internal standard. Mass spectra were recorded on micromass GCT-MS mass spectrometer. UV-vis absorption spectra were recorded by a Shimadzu UV-3600 spectrophotometer. The fluorescent spectra were recorded by a Hitachi F-7000 spectrometer. The FT-IR spectra are obtained on the Nexus-380 FT-IR spectrophotometer with KBr pellet as the blank, in the range of 4000-400 cm^{-1}.

For Z scan measurement, the source was an optical parametric amplifier pumped by a Ti:sapphire amplifier and tunable in the spectral range of 680 nm to 1080 nm delivering 140 fs pulses at a repetition rate of 1 kHz. The input laser beam was focused to a spot size of 1.1 mm with a 5 cm focal length convex lens. A quartz cuvette of 1 mm thickness was used to hold the sample. The sample was translated using a linear translation stage interfaced to a computer. The *fs* degenerate pump-probe experiments were performed near 740 nm for PyAnOH-DMSO solution and 840 nm for PyAnOH-Ag-DMSO suspension. The pump pulse energy was 500 mW while the probe pulse energy was 150 mW.

$$Tz = \sum_{m=0}^{\infty} \frac{[-q(z)]^m}{(m+1)^{3/2}} \quad q(z) = \frac{\beta I_0 L_{eff}}{[1+(z/z_0)^2]\alpha} \qquad \text{(Equation 1)}$$

Where Z_0 was the diffraction length of the beam, I_0 was the intensity of the light at focus, L_{eff} was the effective length of the sample, α was the linear absorption coefficient at the wavelength used.

$$\delta = h\upsilon\beta \times 10^{-3}/N_A d \qquad \text{(Equation 2)}$$

where h was the Planck's constant 6.63×10^{-34} J·s, υ was the frequency of input intensity, N_A was the Avogadro constant 6.02×10^{-23}, and d was the concentration of the sample. "0 mm" is defined as light spot focus.

S2 Characterization of silver NPs, PyAnOH and PyAnOH-Ag hybrid

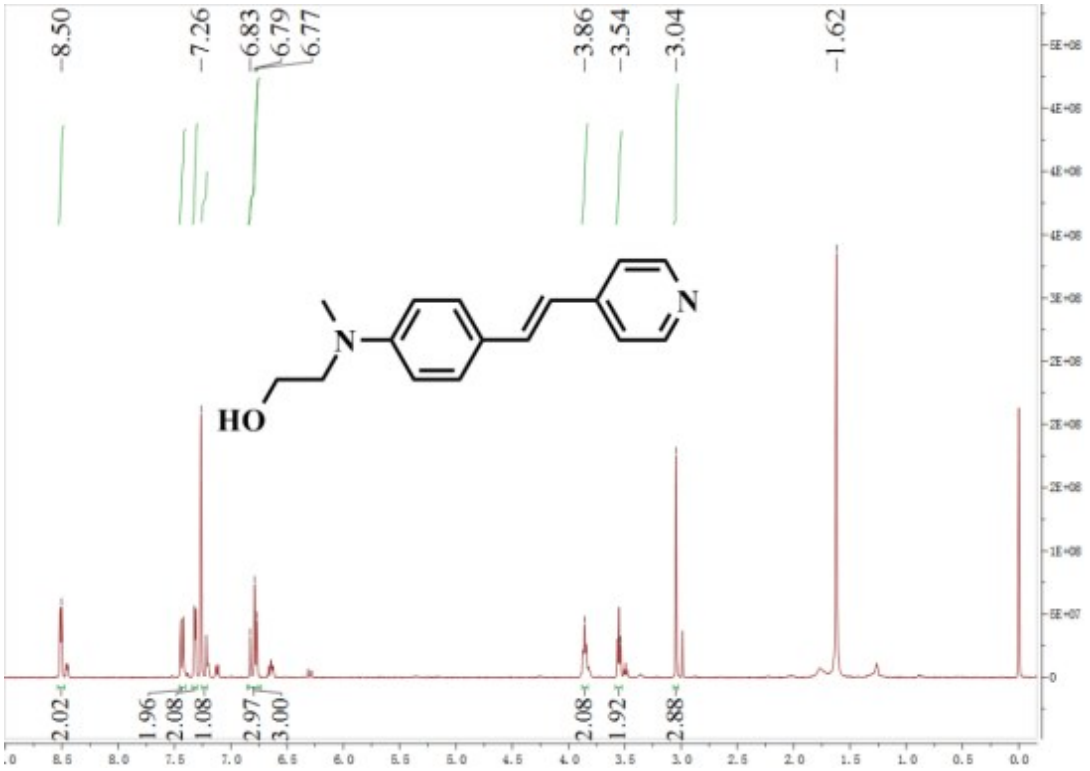

Figure S1. [1]H NMR spectrum of PyAnOH

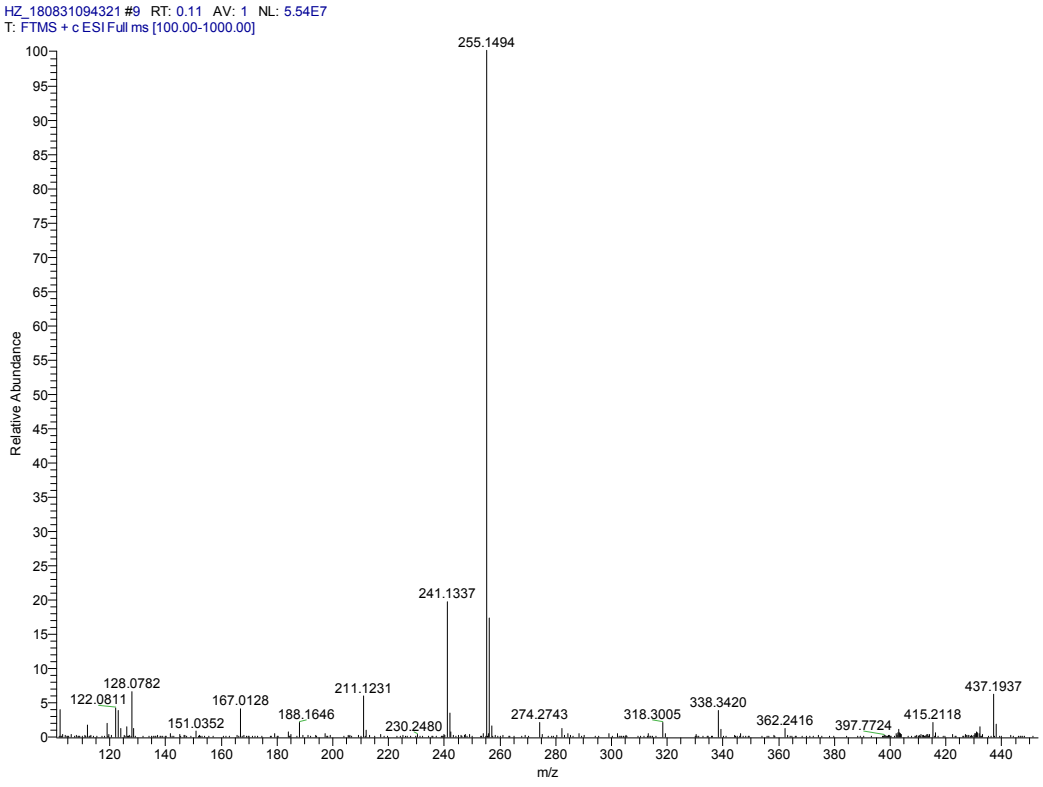

Figure S2. ESI-MS spectrum of PyAnOH.

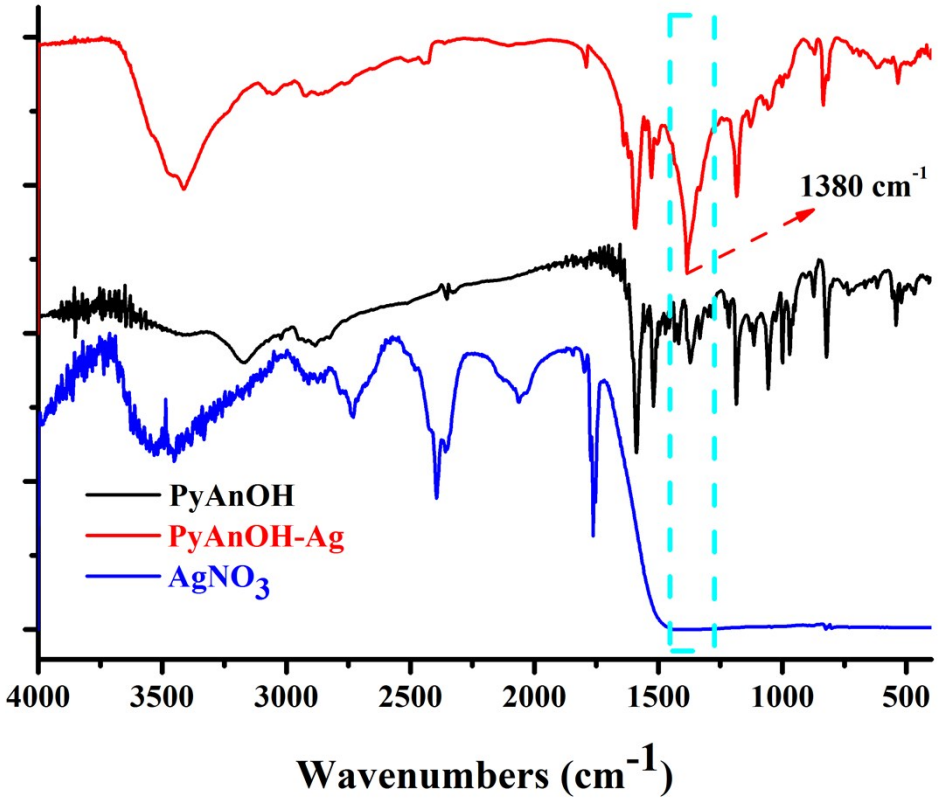

Figure S3. FT-IR spectra of PyAnOH, PyAnOH-Ag and $AgNO_3$ respectively.

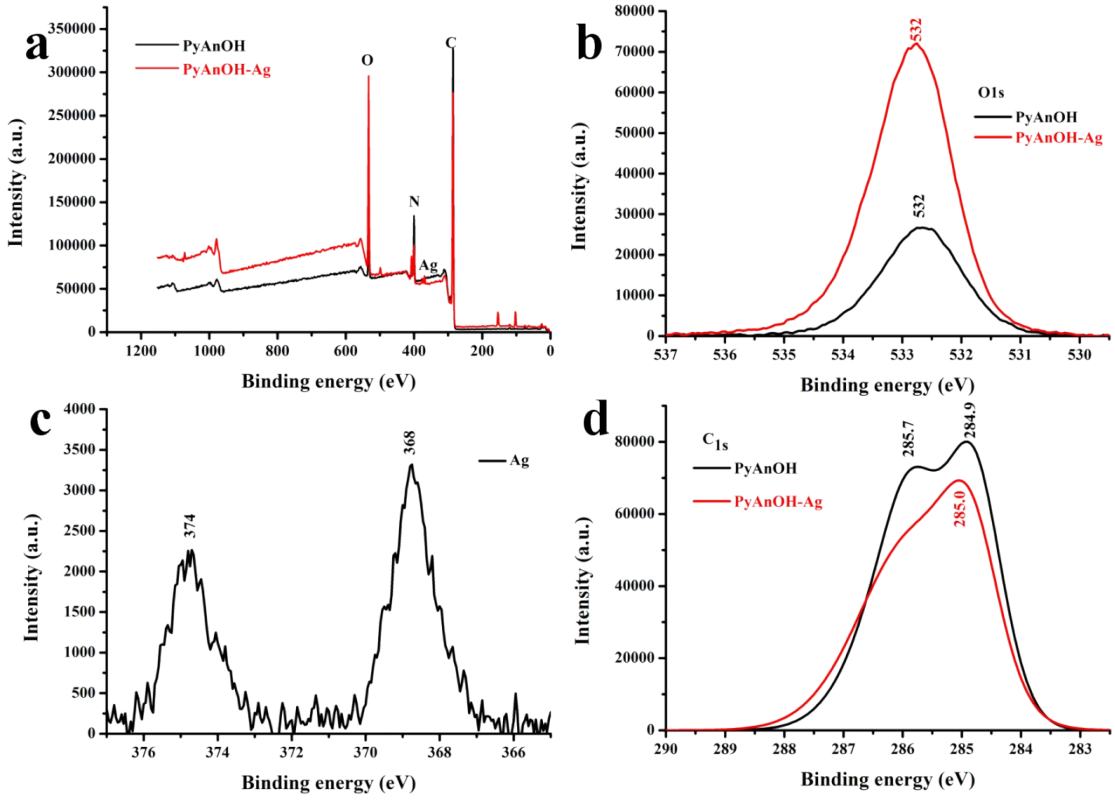

Figure S4. (a) XPS spectra for survey scan of PyAnOH, PyAnOH-Ag. XPS spectra for O_{1s} (b), Ag (c) of PyAnOH, PyAnOH-Ag. (d) XPS spectra for C_{1s} of PyAnOH-Ag

Table S1 Atomic content in PyAnOH-Ag

atom	N	O	Ag	C
atomic percentage (%)	11.2	20.2	0.18	68.42

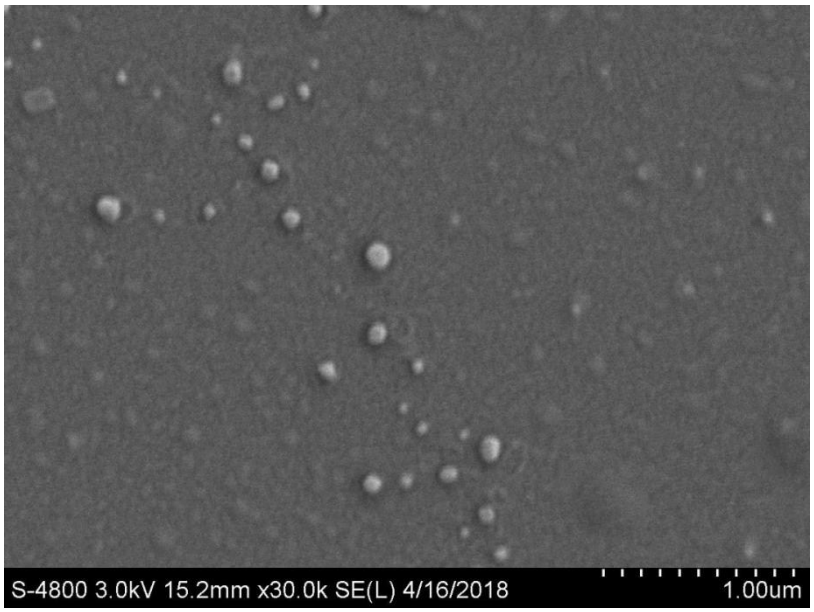

Figure S5 SEM image of free PyAnOH

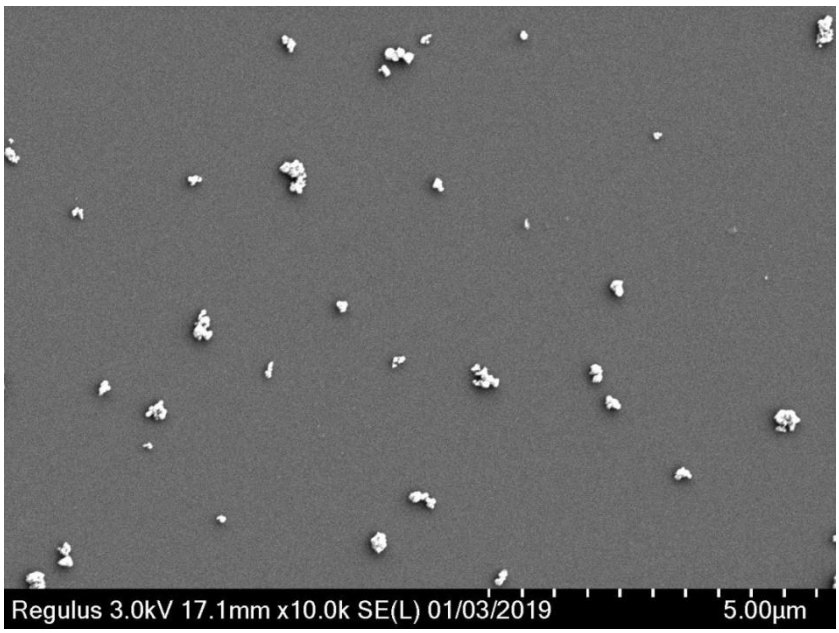

Figure S6 SEM image of pure Ag nanoparticle

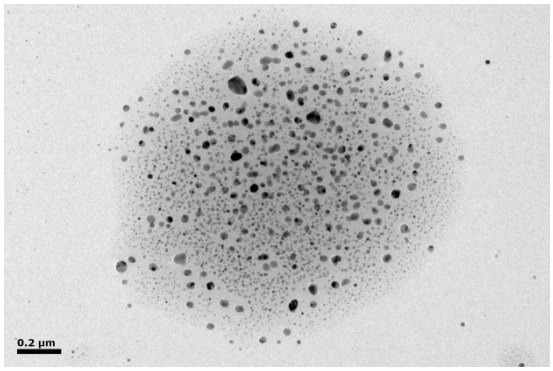

Figure S7 The low-magnification TEM image of PyAnOH-Ag hybrid

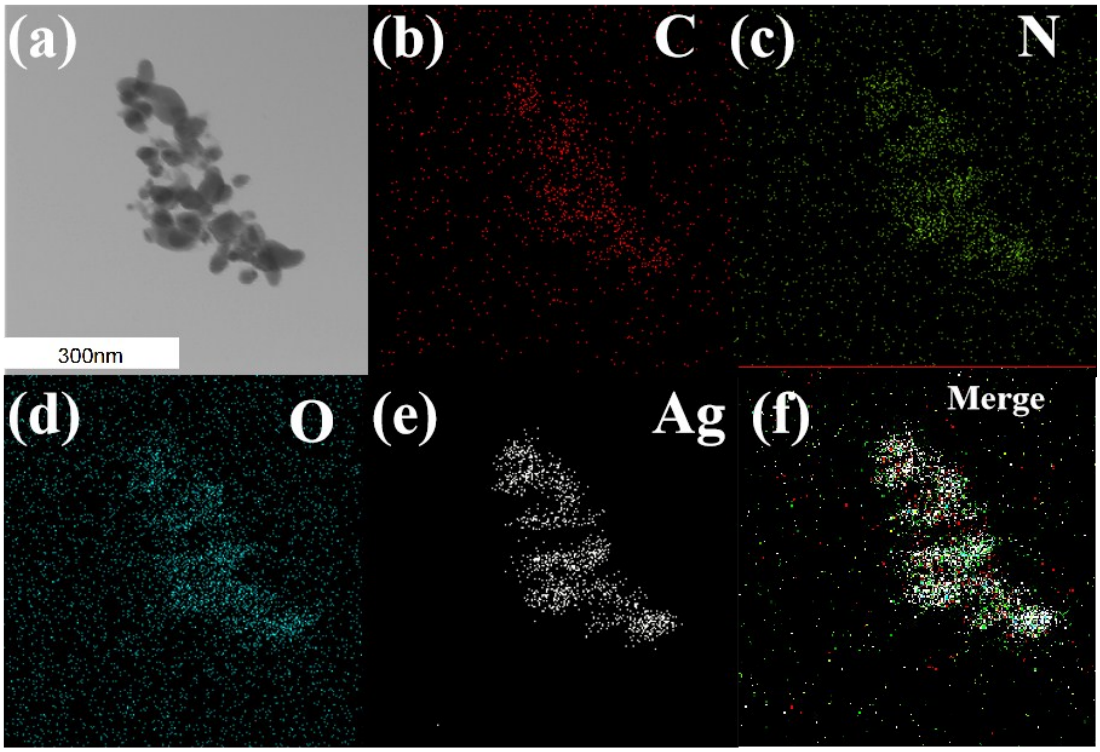

Figure S8. (a) TEM image of PyAnOH-Ag hybrid, (b–e) the mapping images of C, N, O, Ag elements, respectively, and (f) the merge of elemental mapping image of PyAnOH-Ag hybrid with enhanced signal/noise ratio.

S3. Linear/nonlinear optical properties of PyAnOH and PyAnOH-Ag

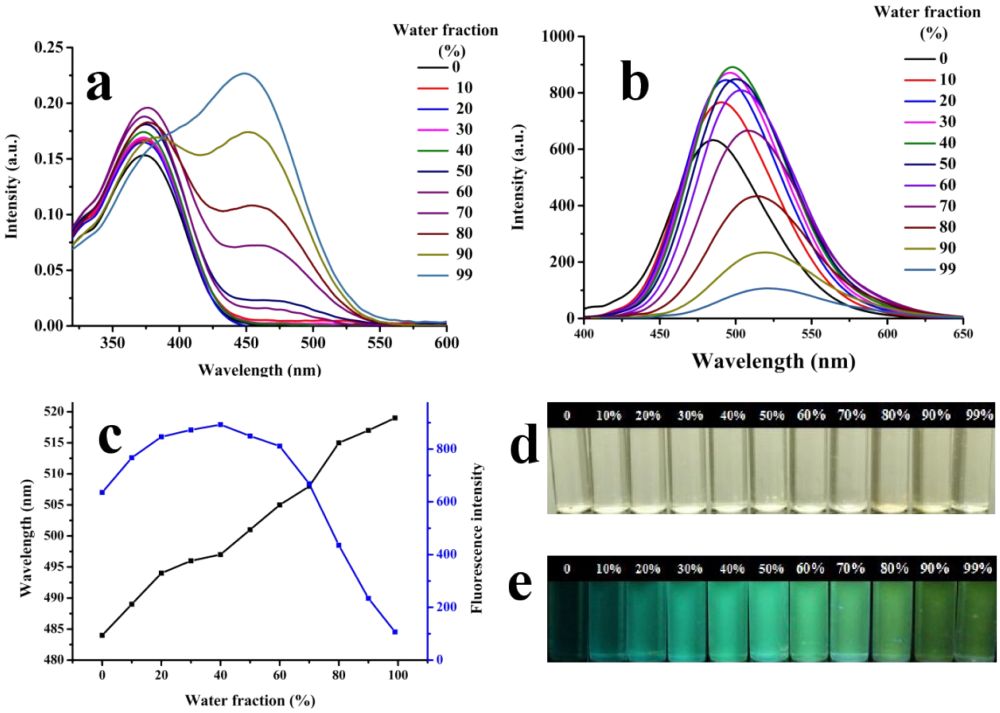

Figure S9. (a) UV-Vis absorption and (b) Fluorescent spectra of PyAnOH (1.0×10^{-5} mol·L^{-1}) in DMSO-H_2O mixtures with different water volume fractions. (c) The effect of water volume fraction on the maximum emission intensity and wavelength of PyAnOH in DMSO-H_2O. (c) Photographs of PyAnOH (1.0×10^{-5} mol·L^{-1}) in daylight and under a lamp (365 nm) at DMSO-H_2O mixtures, respectively.

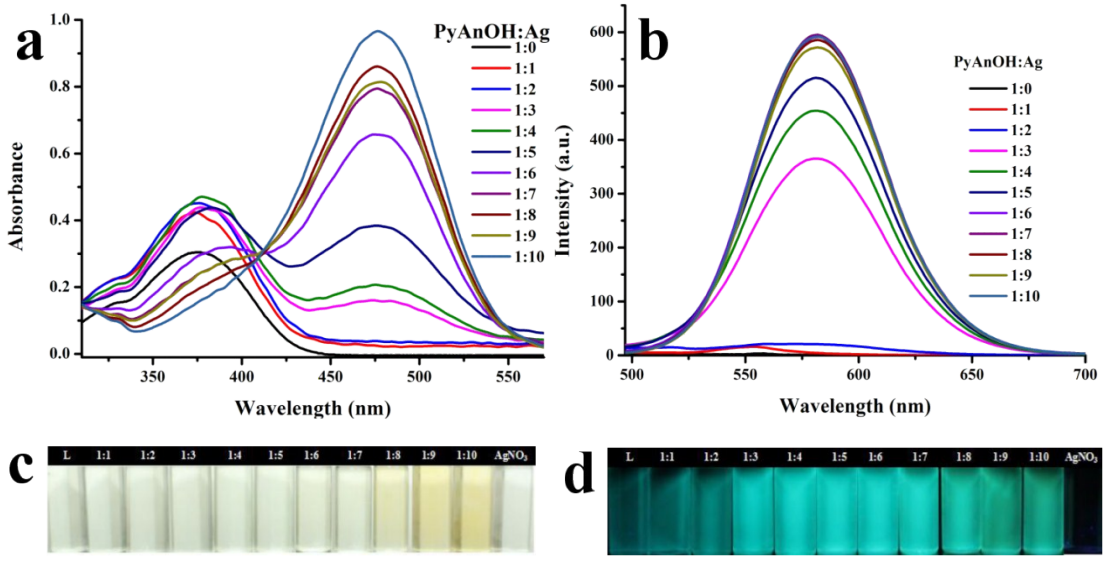

Figure S10. (a) UV-Vis absorption and (b) Fluorescent spectra of the molar ratio of PyAnOH (1.0×10^{-5} mol×L^{-1}) to Ag from 1:1 to 1:10 in DMSO; (c-d) Photographs of the molar ratio of PyAnOH to Ag from 1:1 to 1:10 in daylight and under a 365 nm UV lamp, respectively.

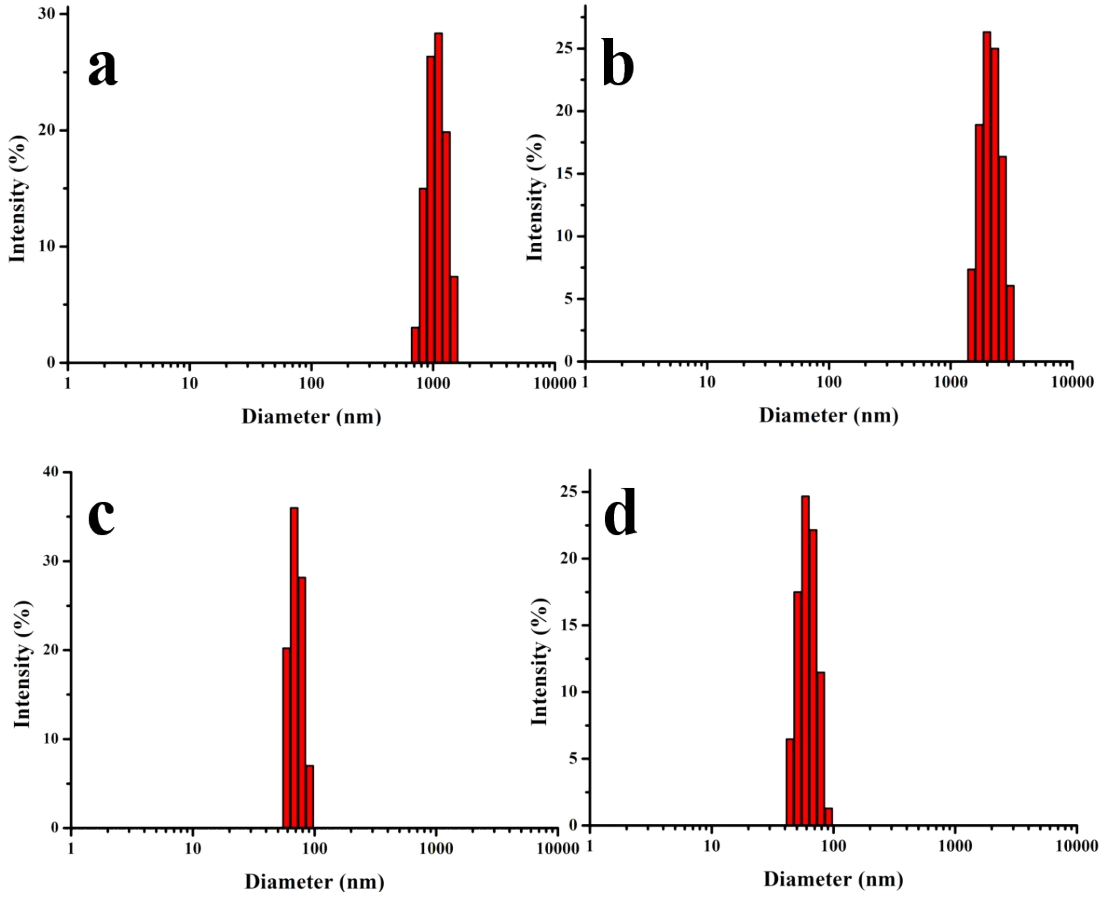

Figure S11. DLS size profiles of PyAnOH in DMSO-H_2O mixed solvent. The water fraction is 0% (a). 40 % (b), 70 % (c) and 99 % (d), respectively.

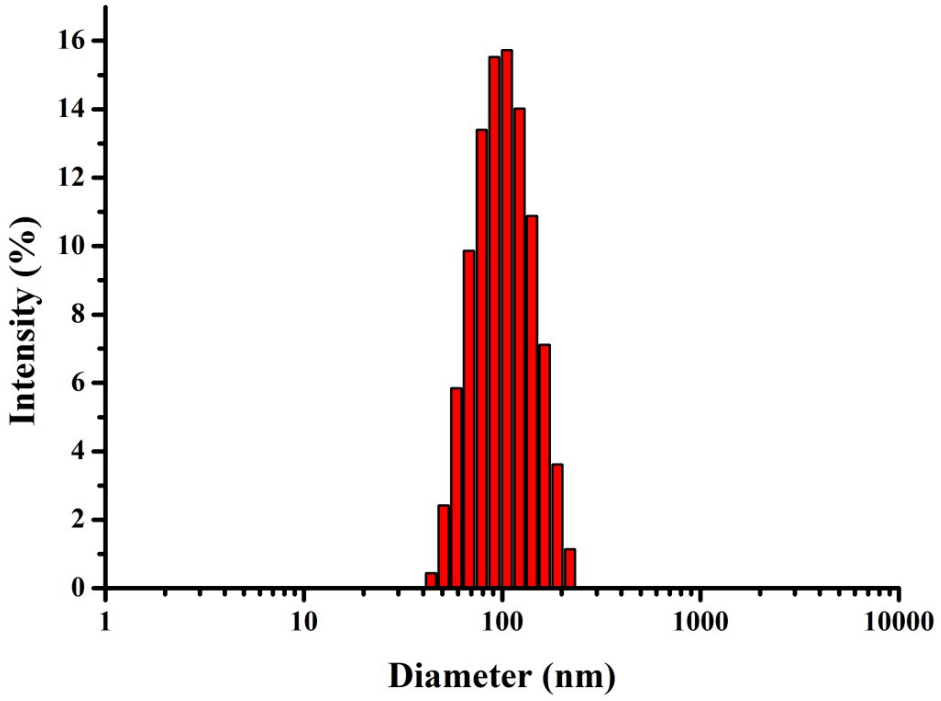

Figure S12. DLS size profiles of PyAnOH-Ag in EtOH

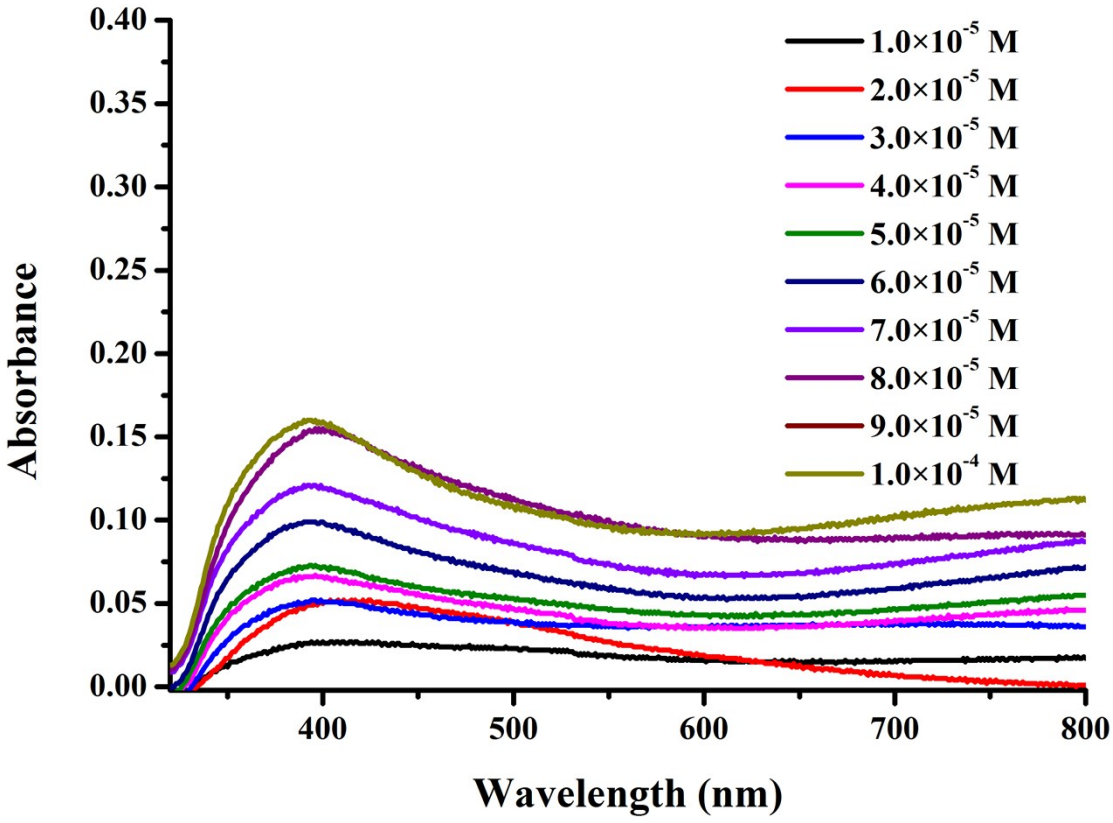

Figure S13. UV-Vis absorption spectra of pure silver nanoparticles (1.0×10^{-5}-1.0×10^{-4} mol·L^{-1}) in EtOH

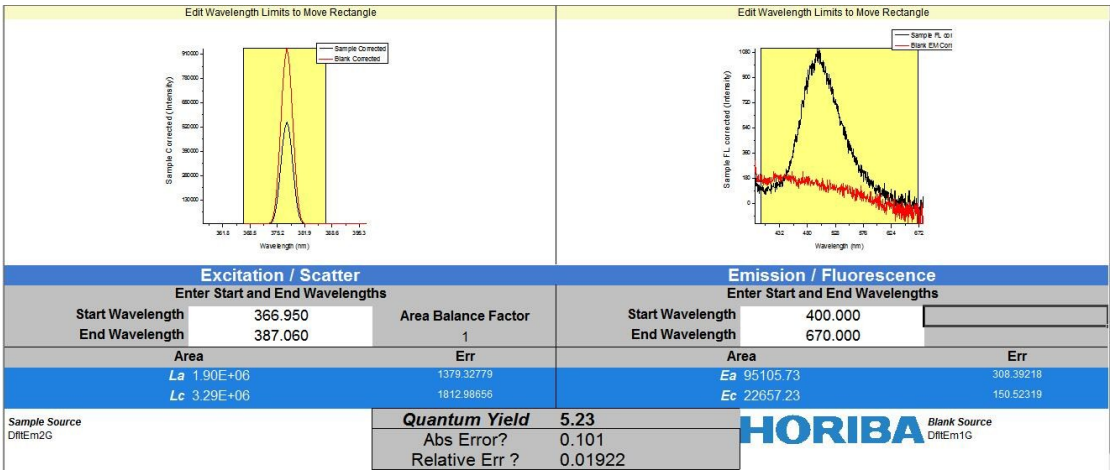

Figure S14. Fluorescent quantum yield of PyAnOH in DMSO

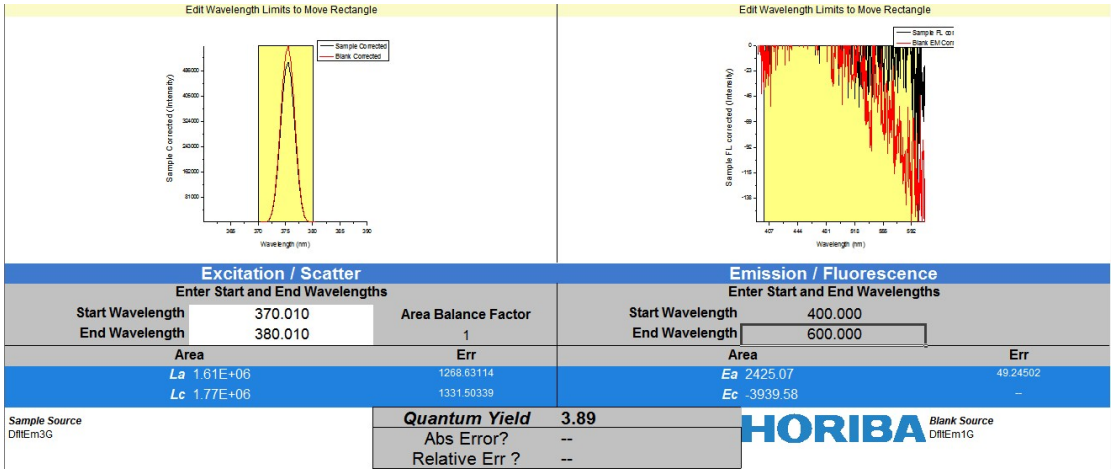

Figure S15. Fluorescent quantum yield of PyAnOH-Ag hybrid in DMSO

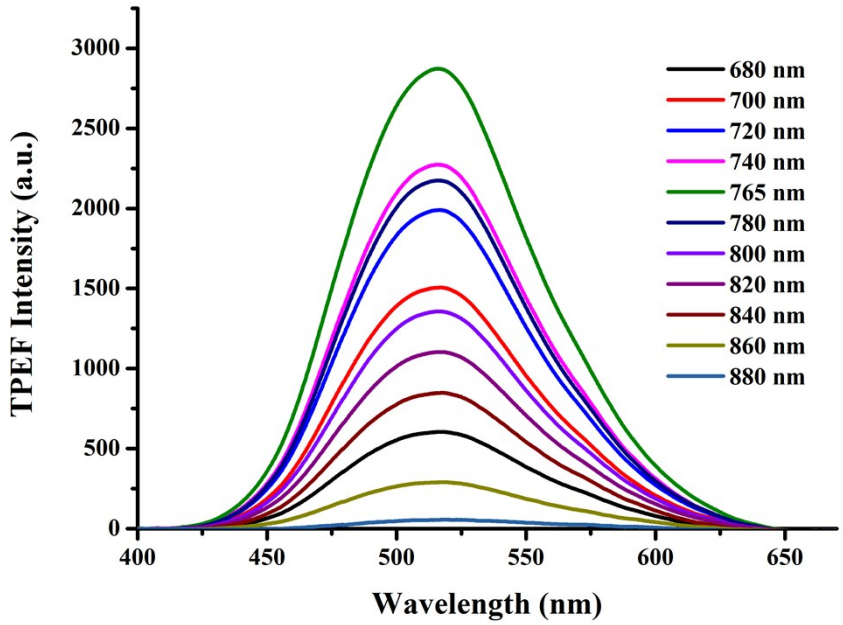

Figure S16. The two-photon fluorescence spectra of PyAnOH in DMSO under different excitation wavelengths

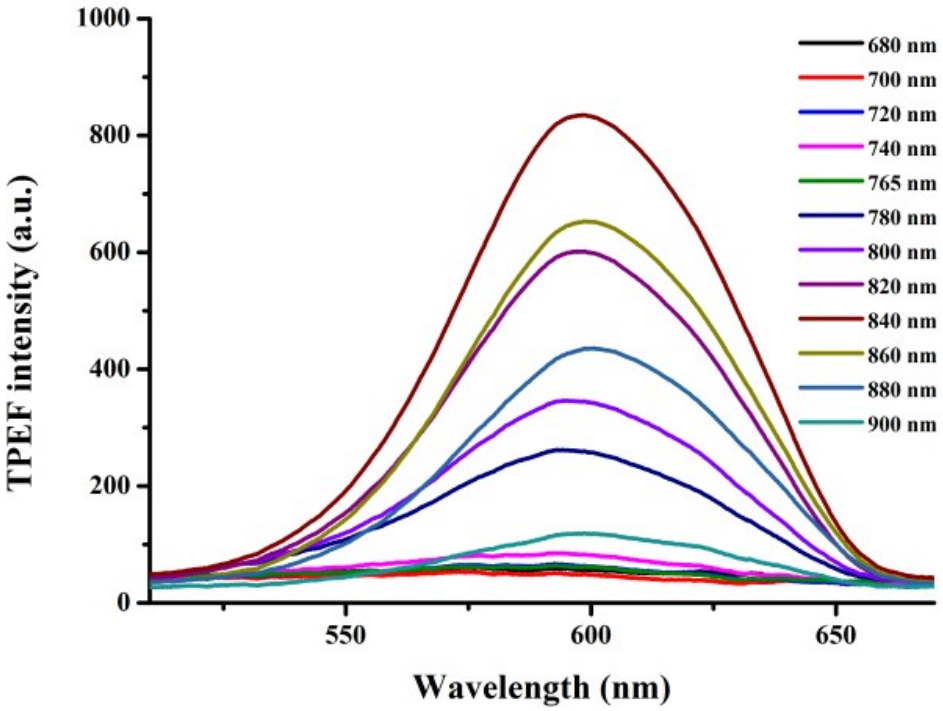

Figure S17. The two-photon fluorescence spectra of PyAnOH-Ag in DMSO under different excitation wavelengths

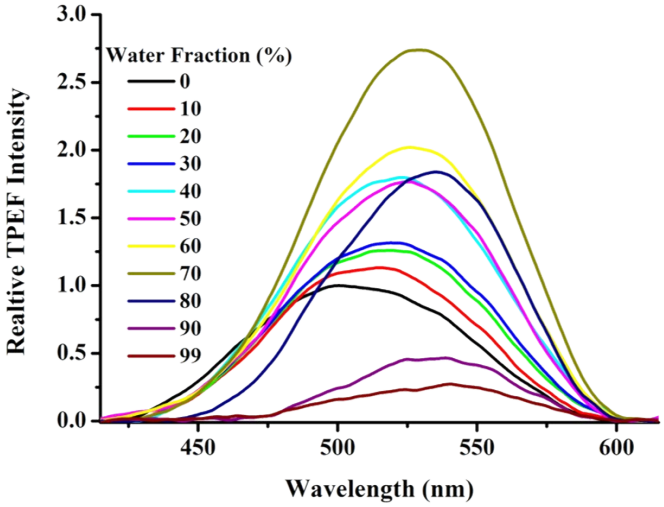

Figure S18. The two-photon fluorescence spectra of PyAnOH in DMSO-H_2O under different water volume fractions (f_w=0~99%).

S4. Confocal co-localization studies of PyAnOH-Ag in cells

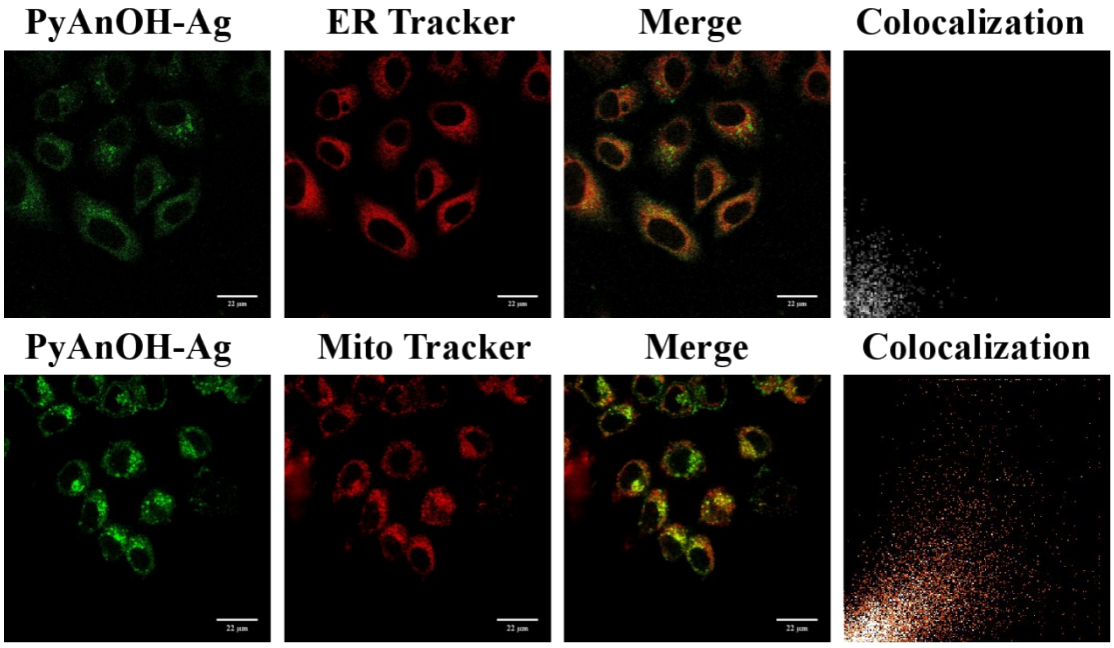

Figure S19. Confocal co-localization studies of PyAnOH-Ag

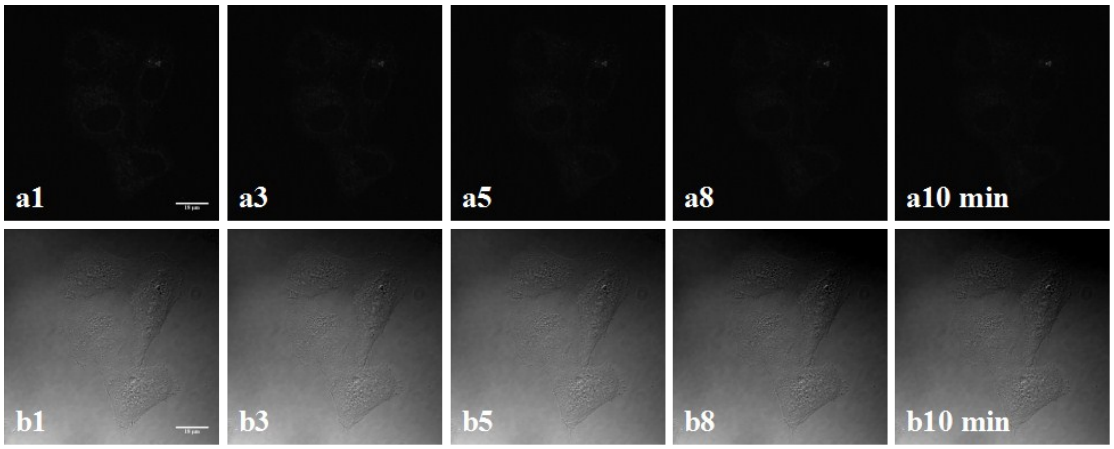

Figure S20 (a-b) Confocal images of two-photon fluorescence and confocal bright field images without PyAnOH-Ag stained HepG2 cells under 840 nm irradiation treatments at different irradiation time.

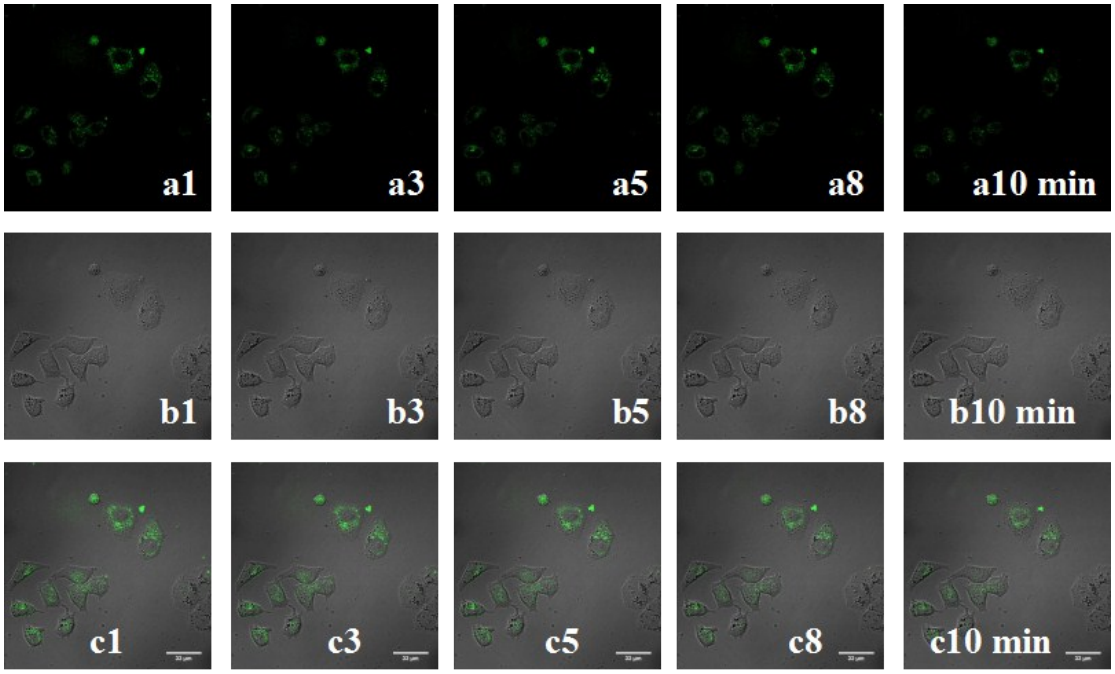

Figure S21 (a-c) Confocal images of one photon fluorescence, confocal bright field and merge images of PyAnOH-Ag stained HepG2 cells under 488 nm laser irradiation treatments at different irradiation time under the dose of 10 μmol·L^{-1}.

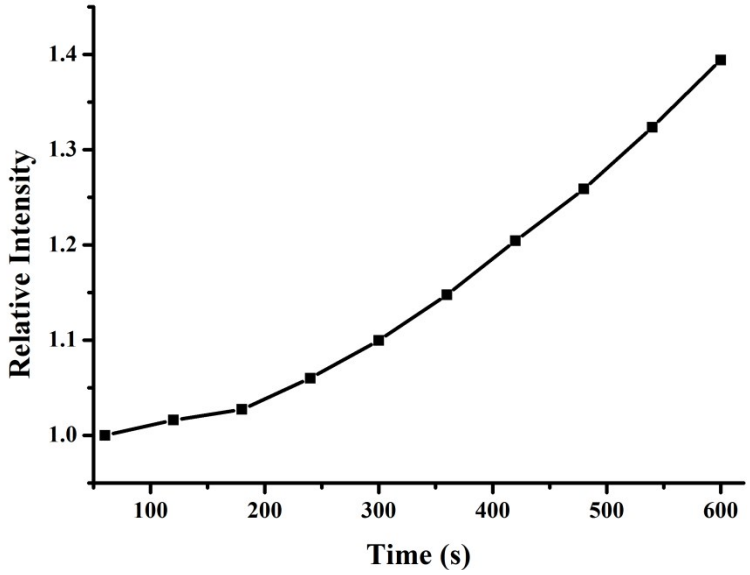

Figure S22 The relative intensity of TPEF emission of PyAnOH-Ag in HepG2 cells during the TP-PTT process.

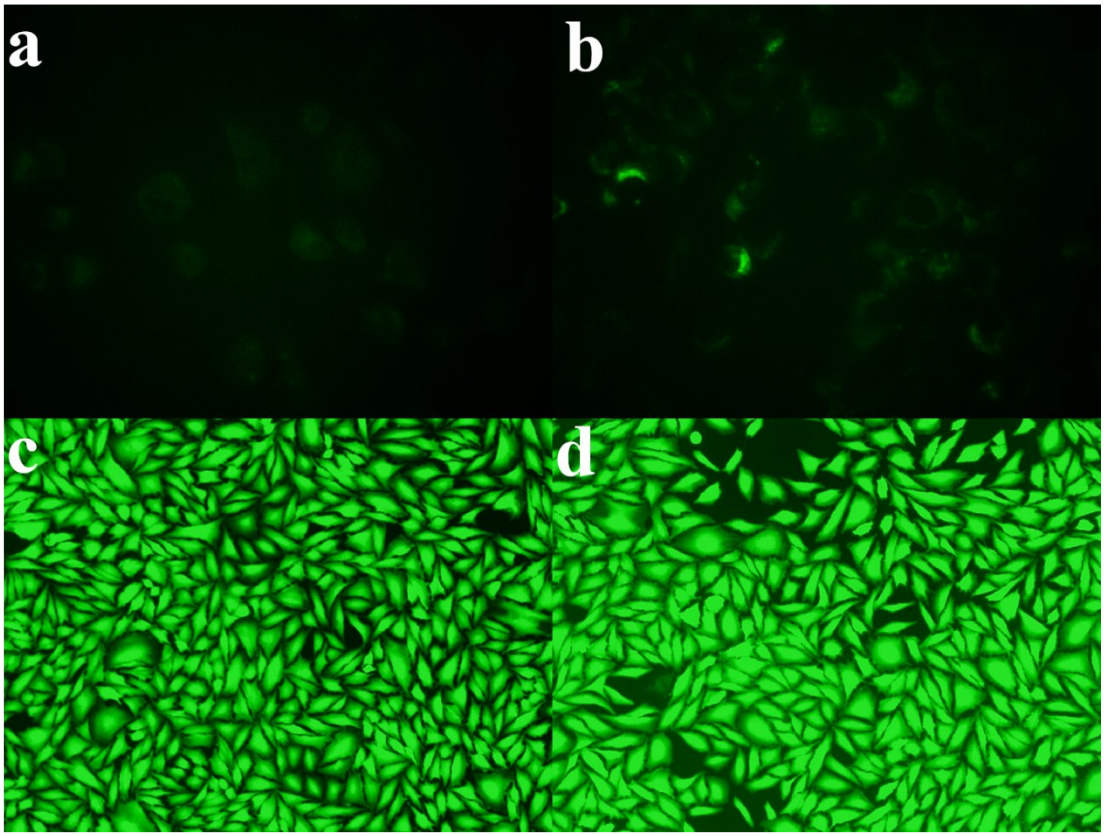

Figuer S23 SPFM imaging of PyAnOH-Ag hybrid in MEF cell with different incubate time, 1 h for (a), 2 h for (b); Cytotoxicity evaluation of PyAnOH-Ag hybrid *via* live/dead assay with different incubate time, 1 h for (a), 2 h for (b).

S5. Biodistribution of PyAnOH-Ag

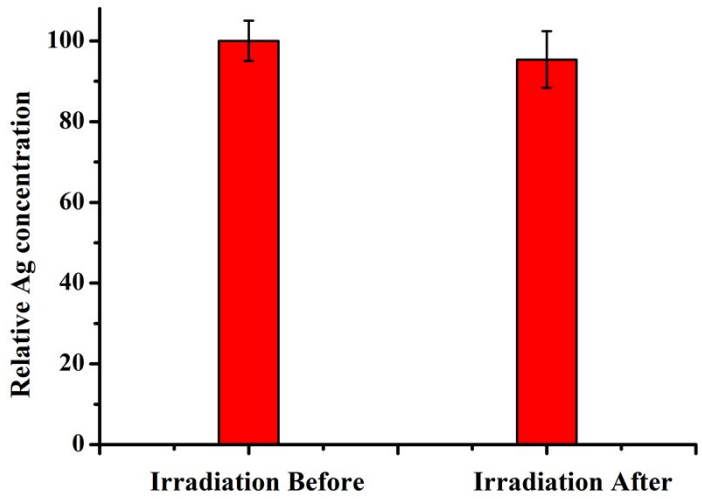

Figure S24. The relative Ag content before and after 10 min irradiation.

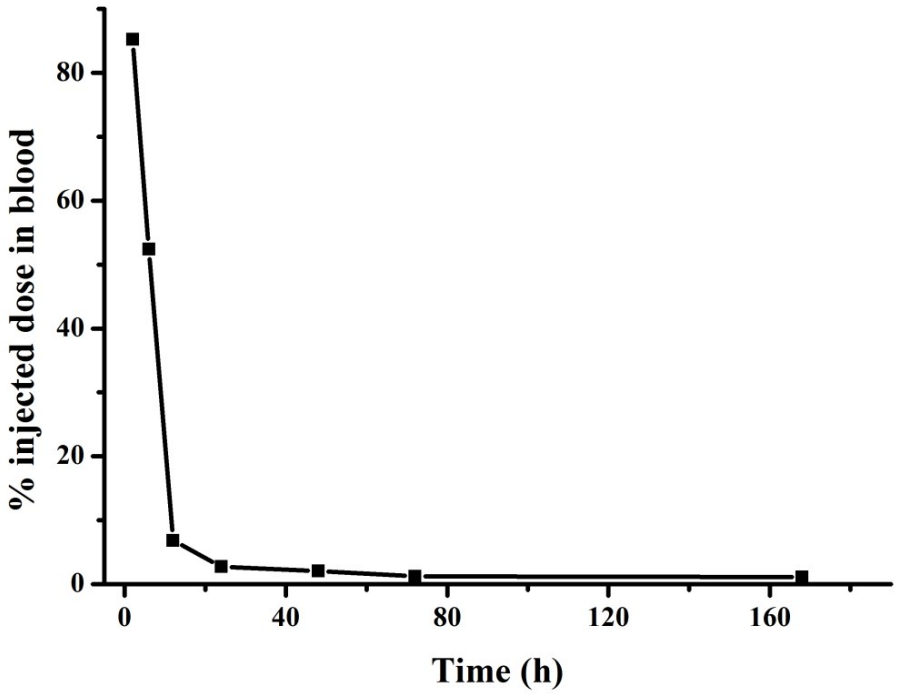

Figure S25 The blood circulation of PyAnOH-Ag in mice during 7 day post-injection

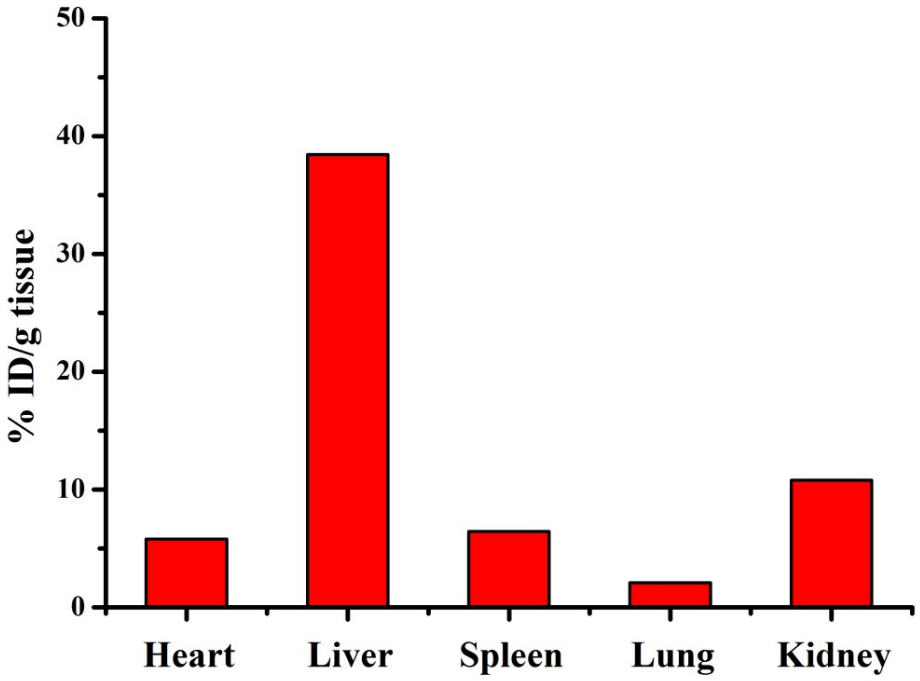

Figure S26 Biodistribution of PyAnOH-Ag measured at 7th day post-injection

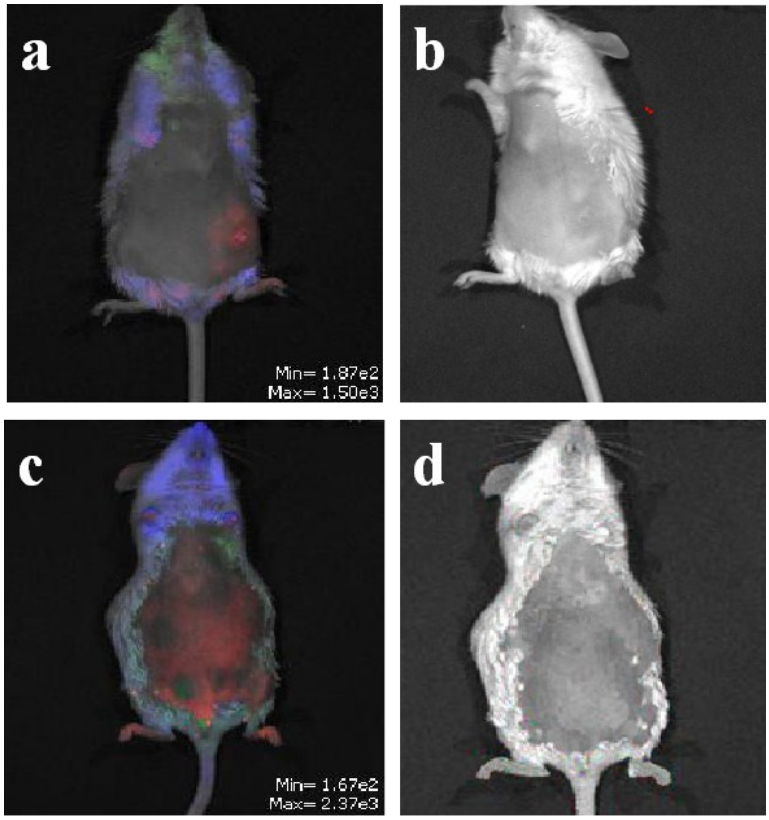

Figure S27 The fluorescence imaging of healthy mice (a-b) and tumor-bearing mice (c-d) after intraperitoneally injection of PyAnOH-Ag

S6 TP-PTT *in vivo*

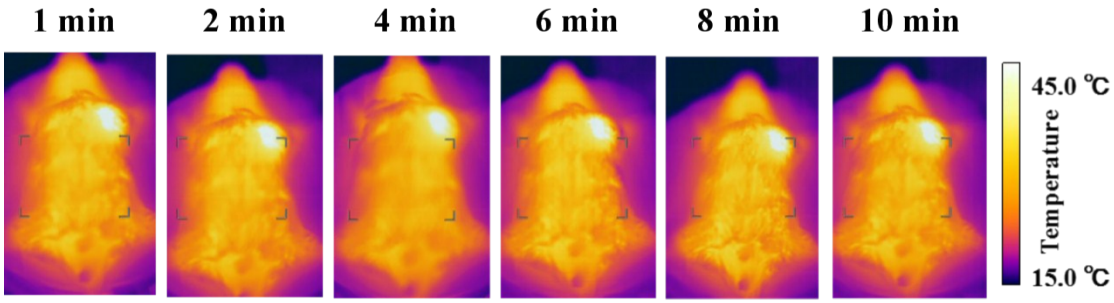

Figure S28. Thermal images of H22-modelled mice injected with PBS under the 840 nm laser irradiation.

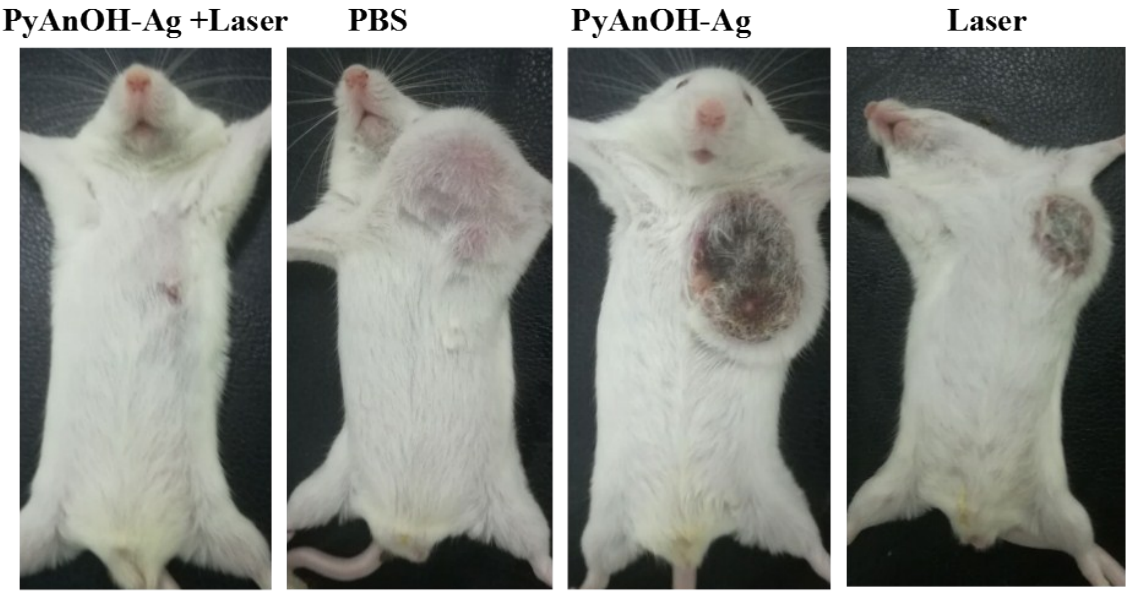

Figure S29. Images of tumor-bearing-mice at 21th day after different treatment methods

Table S2. Comparision of the tumor inhibition ratios of some reported materials for cancer phototheramal therapy

materials	monitoring ability	tumor inhibition ratios	Ref
Gold-nanorods-siRNA	No	79.5% ± 13.0%	S1
self-assembled IR820-PTX nanoparticles	Yes	89.3%	S2
Au-Ag nanourchins	No	almost 100%	S3
folic acid-Janus-type silver mesoporous silica nanoparticles@indocyanine green	Yes	88.9%	S4
S, Se-codoped carbon dots	No	70%	S5
Magnéli-phase titanium oxides	No	almost 100%	S6
PyAnOH-Ag hybrid	Yes	almost 100%	this work

Reference:

S1 B. K. Wang, X. F. Yu, J. H. Wang, Z. B. Li, P. H. Li, H. Y. Wang, L. Song, P. K. Chu, C. Z. Li, *Biomaterials,* 2016, **78**, 27-39.

S2 D. Zhang, J. Zhang, Q. Li, H. L. Tian, N. Zhang, Z. H. Li, Y. X. Luan, *ACS Appl. Mater. Interfaces*, 2018, **10**, 30092-30102.

S3 Z. Liu, L. Cheng, L. Zhang, Z. B. Yang, Z. Liu, J. X. Fang, *Biomaterials*, 201**4**, **34**, 4099-4107.

S4 Z. Wang, Z. M. Chang, M. M. Lu, D. Shao, J. Yue, D. Yang, M. Q. Li, W. F. Dong. *ACS Appl. Mater. Interfaces*, 2017, **9**, 30306-30317.

S5 M. H. Lan, S. J. Zhao, Z. Y. Zhang, L. Yan, L. Guo, G. L. Niu, J. F. Zhang, J. F. Zhao, H. Y. Zhang, P. F. Wang, G. Y. Zhu, C. S. Lee, W. J. Zhang, *Nano Res.*, 2017, **10**, 3113-3123.

S6 G. Ou, Z. W. Li, D. K. Li, L. Cheng, Z. Liu, H. Wu, *Nano Res.*, 2016, **9**, 1236-1243.